Modulation of electrostatic interactions to improve controlled drug delivery from nanogels

Emanuele Mauri, Giulia M.F. Chincarini, Riccardo Rigamonti, Luca Magagnin, Alessandro Sacchetti *, Filippo Rossi *

Department of Chemistry, Materials and Chemical Engineering "Giulio Natta", Politecnico di Milano, via Mancinelli 7, 20131 Milan, Italy

A B S T R A C T

The synthesis of nanogels as devices capable to maintain the drug level within a desired range for a long and sustained period of time is a leading strategy in controlled drug delivery. However, with respect to the good results obtained with antibodies and peptides there are a lot of problems related to the quick and uncontrolled diffusion of small hydrophilic molecules through polymeric network pores. For these reasons research community is pointing toward the use of click strategies to reduce release rates of the linked drugs to the polymer chains. Here we propose an alternative method that considers the electrostatic interactions between polymeric chains and drugs to tune the release kinetics from nanogel network. The main advantage of these systems lies in the fact that the carried drugs are not modified and no chemical reactions take place during their loading and release. In this work we synthesized PEG-PEI based nanogels with different protonation degrees and the release kinetics with charged and uncharged drug mimetics (sodium fluorescein, SF, and rhodamine B, RhB) were studied. Moreover, also the effect of counterion used to induce protonation was taken into account in order to build a tunable drug delivery system able to provide multiple release rates with the same device.

1. Introduction

In the last years a lot of efforts and studies were devoted to the synthesis of novel drug delivery systems consisting of polymeric nanocarriers [1–4]. The need to improve classic drug administration routes like oral, intravenous and intra-arterial was and still is one of the main goals of these researches [5,6]: indeed, while pills and injections have enabled significant medical advances, these methods are inadequate for the delivery of drugs with short half-lives, poor permeability in membranes, and serious toxicity when delivered systemically in large doses. In particular, the main improvement would be the possibility to maintain drug level in plasma at an effective level for a sustained period of time, avoiding under- and over-dosing [7,8]. Moreover, novel drug delivery systems should guarantee: (*i*) drug protection from hostile environment; (*ii*) controlled release in response to environment stimuli like pH or temperature; (*iii*) drug targeting and selectivity to specific organs, tissues or cells thus improving the pharmacodynamic characteristics of the drug [9–11]. Following these objectives and criteria, researchers and companies focused their attention on the design of new smart drug vehicles made of polymeric colloidal dispersions [2,12]. In this framework nanogels (NGs) appear as a promising tool: they are nanosized networks composed by physically or chemically cross-linked polymers and characterized by high biocompatibility and biodegradability. They provide large specific surface, which guarantees the interaction with physiological compartments and enhances stability and bioavailability of the loaded drugs and proteins [13,14]. Despite the good results obtained in many applications, several critical aspects are related to the fact that drug release is mostly driven by pure diffusion mechanism that is very quick due to the high clearance observed *in vivo* [15,16]. The hydrophilic nature of encapsulated drugs and biomolecules is not enough to control the release mechanisms, therefore, the necessity to develop NGs able to delay release rates or allow multiple release kinetics, different from pure-Fickian ones, is very demanding [17,18].

In order to overcome these drawbacks and so attenuate diffusional release of biomolecules Vulic et al. [19] introduced biorthogonal strategies to create an affinity bond between peptide and polymeric network, covalently linking a small protein receptor module to her gel systems. Similar procedures were also followed by several other groups [16,20,21] that used different functionalization strategies to link drugs to polymers. In these cases, drug release is not driven by Fickian diffusion but delayed by the stability or affinity of the bond between drug and polymer: higher the stability and slower the release kinetics. This approach guarantees the controlled and sustained release of drugs/biomolecules on one hand, but on the other hand, the chemical modification of active principles may change their efficacy [19,21,22]. With the aim of

avoiding the formation of covalent bonds between therapeutic compounds and polymers, but taking advantages from the interactions that could take place among solutes and polymers [15,17,23], we decided to consider electrostatic interactions.

In particular in this work we synthesized NGs based on polyethylene glycol and polyethylenimine PEG-PEI, suitable for biomedical applications [24], with different protonation degrees. The colloidal dispersions were characterized in terms of dimensions, polydispersity and ζ-potential and then loaded with two different drug mimetics. The first one was sodium fluorescein (SF), a commonly used drug-mimetic molecule [25–27], chosen for its steric hindrance and its resemblance to many corticosteroids and anti-inflammatory drugs (for example, methylprednisolone, ibuprofen, and estradiol) used in pharmacotherapy. Moreover, SF is a sodium salt like several drugs already listed and in water it is dissociated into fluorescein anion and sodium cation [26]. The second one was Rhodamine B (RhB), drug mimetic with the same dimension of SF, in order to neglect the steric hindrance contribution in the experiments [28,29]. RhB is a neutral molecule at pH = 7.4 and slightly positive at acid pH: this behavior can be found in several amine-based drugs like lidocaine or trandolapril [30]. To validate and confirm the results collected with the charged drug we compared them with release studies performed with rhodamine.

As a significant consequence of this study, it could be possible to tune the delivery of charged therapeutic compounds from NGs, according to specific pharmacological and medical needs, tuning polymer protonation degrees. This strategy is able to guarantee suitable delivery kinetics avoiding chemical modification of loaded drugs/biomolecules.

2. Materials and methods

2.1. Materials

All experiments were performed using the following polymers: polyethyleneimine linear (MW = 2500 Da, by Polysciences Inc., Warrington, USA) and polyethylene glycol 8000 (MW = 8000 Da, by Sigma-Aldrich Chemie GmbH, Deisenhofen, Germany); all other used chemicals were purchased from Sigma-Aldrich (Sigma Aldrich Chemie GmbH, Deisenhofen, Germany). The materials were used as received, without further purification. Solvents were of analytical grade. Synthetized products containing fluorescein sodium salt or rhodamine B were stored at 4 °C in dark. The NMR experiments were carried out on a Bruker AC (400 MHz) spectrometer using chloroform ($CDCl_3$) as solvent, and chemical shifts were reported as δ values in parts per million with respect to TMS as internal standard.

2.2. Synthesis of NG-c^+

Nanogels constituted by PEG and PEI with high cationic charge density, labelled as NG-c^+, were synthetized referring to the modified emulsification-evaporation method [31]. Briefly, PEG was activated using 1,1′-carbonyldiimidazole (CDI) as discussed in our previous work [24] and the modified polymer (200 mg, 0.025 mmol) was dissolved in CH_2Cl_2 (3 ml). PEI (52 mg, 0.021 mmol) was added to distilled water (5 ml), under stirring at 30 °C until complete dissolution. Then, HCl 1 M was added to adjust pH at 4.5. Successively, the organic solution was poured dropwise to PEI solution under vigorous stirring and the resulting mixture was sonicated for 30 min and CH_2Cl_2 was evaporated. The obtained solution was left stirring for 17 h at 25 °C and purified performing a dialysis against aqueous solution at pH 4.5 (using a membrane of M_w cutoff = 3500 Da), prepared from distilled water (2000 ml) and HCl 37% w/w (0.72 ml). Finally, the resulting mixture was lyophilized.

The product was then characterized by ^{1}H NMR analysis and nanogel size and charge were investigated using DLS and AFM techniques.

2.3. Synthesis of NG-u

Nanogels synthetized by PEG and uncharged PEI, named NG-u, were prepared following the procedure illustrated in the previous section, using alkaline conditions both in nanostructure formation and dialysis, instead of acidic ones. In summary, PEI (52 mg, 0.021 mmol) was dissolved in distilled water (5 ml) and the solution was carried to pH 10.5 with NaOH 1 M. The organic solution of PEG bis-activated CDI was added dropwise to PEI alkaline system and sonicated for 30 min. Then the organic solvent was removed under reduced pressure and the system left stirring for 17 h at 25 °C. The resulting solution was dialysed against aqueous solution at pH 10.5, consisting of distilled water (2000 ml) and NaOH 1 M (2 ml) and lyophilized. The system was analyzed through ^{1}H NMR spectroscopy, while DLS and AFM gave information about size and ζ-potential of the nanogels NG-u.

2.4. Nanogel characterization

The hydrodynamic diameters as well as ζ-potentials and the polydispersity index of nanogels NG-c^+ and NG-u were determined by dynamic light scattering (DLS) measurements using a Zetasizer Nano ZS from Malvern Instruments. The reported data are an average value of three measurements of the same sample: for NG-c^+, the sample was dissolved in acidic solution (pH = 4.5); whereas NG-u one was dissolved in alkaline solution (pH = 10.5). Atomic force microscopy (AFM) analysis was performed using a NT-MDT Solver Pro instrument operating in non-contact mode with silicon tips.

Samples were prepared by dropping nanogel latexes onto silicon substrate and drying. AFM images on 1 × 1 μm areas were recorded for the preliminary morphologic evaluation; 500 × 500 nm image were then cropped and height line profile performed for single nanostructure. The evaluation of the surface morphology and nanogel size were obtained by flattening of the images (first order) using NTMDT software.

2.5. Loading of nanogels with fluorescein and rhodamine B

Two drug mimetic solutions were prepared dissolving, separately, SF and RhB in distilled water (both solutions at concentration of 1 mg/ml). Lyophilized nanogels NG-c^+ and NG-u were independently suspended in aqueous solution (20 mg/ml). Then, 1 ml of drug mimetic solution was added dropwise (1 ml/min) to 1 ml of nanogel solution under stirring and the system was left to stir for 17 h at 25 °C, in dark. Following this procedure, we performed the loading of SF and RhB within the network of each type of synthetized nanogel: fluorescein was entrapped within NG-c^+ and NG-u and, in the same manner, other samples of NG-c^+ and NG-u carried rhodamine. Successively, loaded nanogels were dialyzed (membrane M_w cutoff = 3500Da) against aqueous solution in order to remove free molecules. Loading efficiency (% loading) was calculated referring to the equation:

$$\%\ \text{loading} = \frac{\text{drug entrapped within NGs}}{\text{initial amount loaded}} \cdot 100 \quad (1)$$

2.6. In vitro drug delivery

Drug release mechanism was investigated in two different release environments: one at pH 7.4 using a phosphate buffered saline solution (PBS), and the other at pH 4.5. In details, each nanogel sample was placed in excess of PBS and in excess of acidic solution (2.5 ml) and aliquots (3 × 100 μl) were collected at defined time points, while the sample volume was replaced by fresh solution, in order to avoid mass-transfer equilibrium with the surrounding release environment. The experiments were performed at 37 °C. Percentages of released SF and RhB

were then measured by UV spectroscopy at a specific wavelength, respectively $\lambda = 485$ nm and $\lambda = 570$ nm.

2.7. Synthesis of NG-p^+

The study of counterion effect on NGs protonation was performed through the synthesis of nanostructures in phosphoric acid media. Referring to Section 2.2, PEG activated CDI was dissolved in CH_2Cl_2, whereas PEI was dissolved in an aqueous solution at pH 4.5 prepared using H_3PO_4 85% solution. Then the organic phase was added dropwise to the aqueous one, sonicated and CH_2Cl_2 removed under vacuum. After stirring for 17 h at room temperature, synthetized nanogels were dialysed against aqueous H_3PO_4 solution at pH 4.5 and finally lyophilized, as the NG-u and NG-c^+ samples. The obtained nanosystems were labelled as NG-p^+, referring to the used phosphoric acid.

2.8. Statistical analysis

Where applicable, experimental data were analyzed using Analysis of Variance (ANOVA). Statistical significance was set to p value <0.05. Results are presented as mean value $\pm$ standard deviation.

3. Results and discussion

3.1. Chemical characterization

The presence of charged or ionizable groups on a polymer chain offers the opportunity to control its physical properties such as solubility, viscosity, tendency to adsorb surface components, cytotoxicity, biocompatibility and charge density by changes in external variables as pH or ionic strength [32]. PEI high charge density is due to the protonation of its amino groups in biological environments: a relationship between the pH value of the solution and the polymer positive charges has been evaluated, showing that the highest PEI protonation degree is at pH 4.5, whereas it is effectively uncharged in alkaline condition (pH = 10.5) [33–35]. In our procedure, PEI was first dissolved in acidic or basic solution to achieve the desired charge density, according to the experimental aims; therefore, the synthesis of NGs positively charged was performed maintaining pH at 4.5 (strongly protonated PEI), while uncharged NGs were produced at high pH value, in order to neutralize the charge on PEI nitrogen atoms. The approach used to prepare the nanostructures involved the cross-linking between activated PEG and PEI in a dichloromethane-in-water emulsion [36]. After completion of the polymeric conjugation, the organic solvent was removed and nanogels were allowed to form and maturate in aqueous medium, at acid or alkaline pH to preserve the electrostatic contribution of the reagent PEI within the network. The maturating phase is important to guarantee the maximum efficiency of the cross-linking reaction, which at high stages of conversion can be limited by the polymeric chain entanglements during nanoparticle formation [37]. Then, the crude suspension was purified by dialysis to remove by-products and unreacted polymers and lyophilized to obtain white solid material capable to be readily swelled and dispersed in aqueous solution.

From the ^{1}H NMR spectroscopy, PEG chain peaks were identified in the range 3.75–3.57 ppm and PEI signals could be recognized in the range 2.95–1.85 ppm; while the signals found at 4.11 ppm and at 3.40 ppm correspond, respectively, to the two methylene protons of PEG and PEI monomer forming the carbamate bond. This confirmed that the cross-linking reaction occurred between the polymer chains. We also observed that no signals shifts were detectable comparing the NMR spectra of NG-c^+ and NG-u samples: this suggested that the different PEI protonation degree does not alter the characteristic signals of products in ^{1}H NMR analysis. The composition of nanogel was determined in terms of polymeric molar ratio, through estimation of the integral values of PEG and PEI characteristic peaks and resulting in a PEG:PEI ratio equal to 2:1 for NG-c^+ sample and 1:1.2 for NG-u system. Therefore, we were able to synthetize a tool that could be modulated in terms of electrostatic interaction against the specific nature of biomedical application, also resulting in a different chemical composition of the network.

3.2. Physical characterization: nanogel size and charge

Nanogel size has a significant impact on active or passive cellular internalization and intracellular localization. Once they have entered into a biological system, NGs come in contact with a huge variety of biomolecules generating size- and charge-dependent interactions [38,39]. The cytocompatibility and the therapeutic effects of these nanostructures depend on the cellular membrane response toward their morphology and their cationic or anionic nature. Dynamic light scattering (DLS) is a commonly used technique to evaluate nanoparticle size in suspension. The measured hydrodynamic diameter reflects the dimension of the nanogel including a layer of surface-bond solvent. Sizes and charges of synthetized NG-c^+ and NG-u are reported in Table 1.

Diameter of NG-c^+ nanogels was significantly smaller than NG-u systems, characterized by size reaching the micron scale. Furthermore, the first ones presented a positive surface charge, while the latter could be considered as a neutral carrier. The difference in size could be justified evaluating the corresponding ζ-potential: PEI high positive charge density might affect nanogel formation. Its chains were able to interact with each other in a repulsive way, preferring the reaction with the uncharged PEG chains: in this way, the synthesis of smaller nanosystems seemed to be encouraged than the formation of larger structures occurring without preferential interactions among the end-groups of the polymers. Indeed, NG-u were composed by polymers with protonation degree equal to zero and the cross-linking between PEI and PEG, performed at alkaline condition, was not influenced by electrostatic interactions. This probably gave rise to larger nanostructures where the diameter was the optimal distance of steric hindrance between the reactive polymer chains. Morphology and size distribution was also quantified by using atomic force microscopy (AFM), as showed in Fig. 1. All the samples showed spherical morphology with a smooth surface and diameter of about 180 nm for NG-c^+ and 500 nm for NG-u. Nanogel sizes observed by AFM were less than those measured using DLS. This variation between AFM and DLS measurements is due to the difference in the sample processing [20,24,40]. In DLS, particle size analysis recorded the hydrodynamic diameter, and so the slight increase in size observed is due to the swelling of the nanogels. The latter could not evaluate in AFM data. In addition, this problem was not present with hydrophobic polymeric nanoparticles synthesized by our group and presented in previous work [41]. In that case, the complete accordance between AFM and DLS was due to the fact that in that system, the swelling phenomenon was negligible. Referring to the physical characterization, the dimensional difference between NG-c^+ and NG-u could affect the aim of the final application, in particular the cellular uptake efficiency and kinetic, and the internalization mechanism.

NG-c^+ samples, according to their size of 180 nm, could be suitable for active or passive cellular internalization, also carrying drugs through the cell membrane and allowing a therapeutic subcellular distribution; otherwise, the uptake of NG-u appeared as more difficult (500 nm) and, in this case, the use of this type of nanogel could be appropriate to maintain the loaded biomolecules into the extracellular media, avoiding any interactions with cell membrane receptors and showing the curative effects outside the cells.

Table 1
Size and charge of the synthetized nanogels measured with DLS.

Nanogel	Diameter (nm)	Polydispersity index (–)	ζ-Potential (mV)
NG-c^+	220	0.270	17.00
NG-u	830	0.217	0.01
NG-p^+	448	0.306	18.10

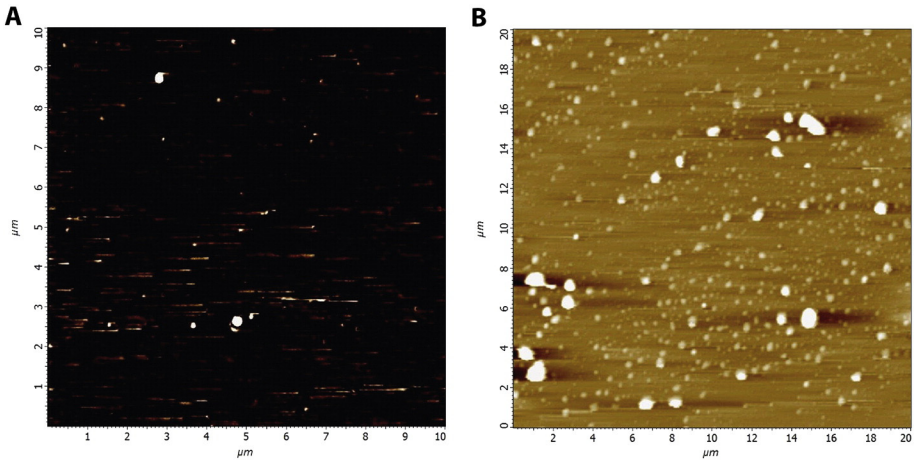

Fig. 1. AFM images of nanogels prepared with different protonation degree: (A) NG-c^{+}, (B) NG-u.

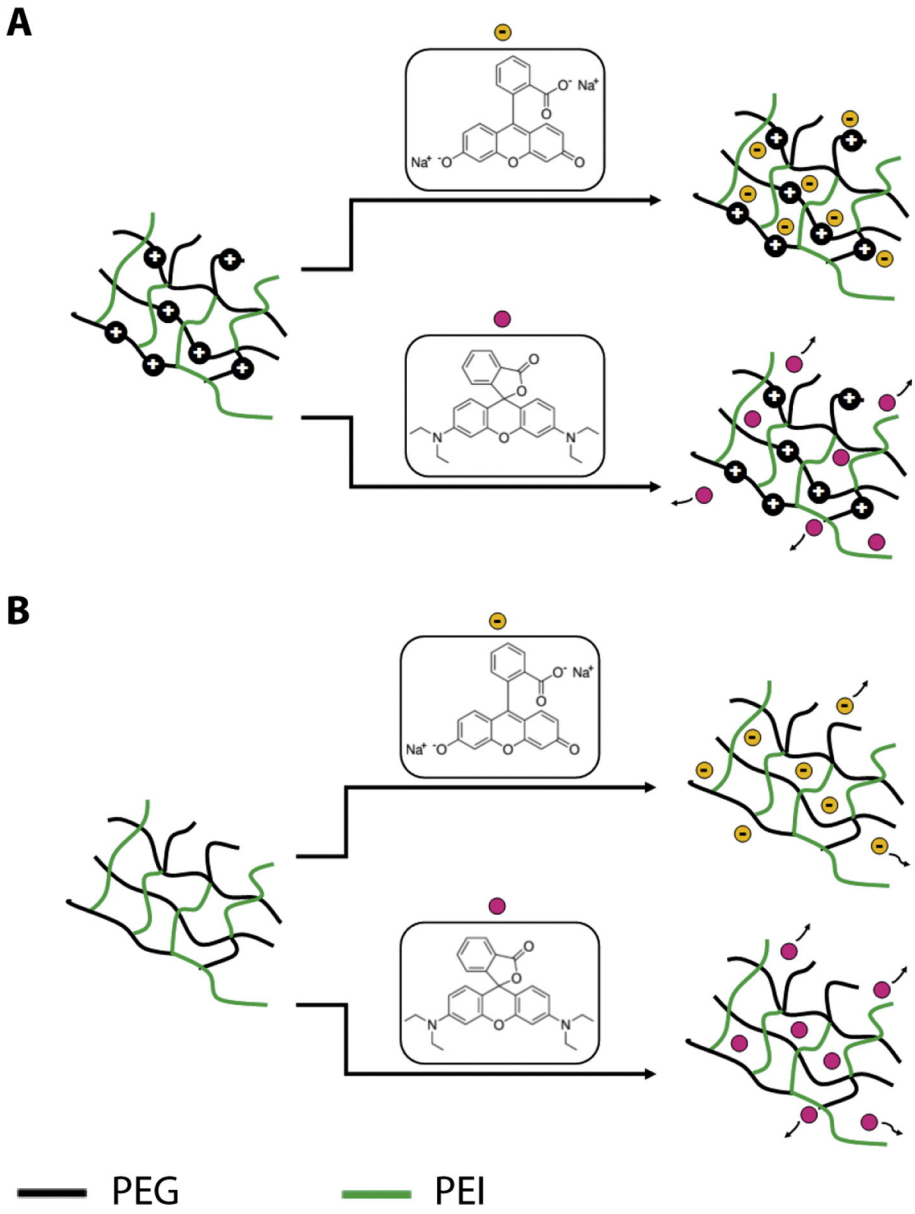

Fig. 2. (A) NG-c^{+}, presenting a positive charge, is able to attract and retain negatively charged drugs (yellow dots, SF) while is not able to retain neutral molecules (pink dots, RhB). (B) NG-u cannot interact with drugs (either charged or neutral) and so their release is not influenced by polymer-drug interactions. (For interpretation of the references to color in this figure legend, the reader is referred to the web version of this article.)

3.3. Tuning drug loading and release by modifying electrostatic interactions

We tested the release of an ionic (SF) and a neutral (RhB) drug mimetic from NG-c$^+$ and NG-u delivery systems. Fig. 2 shows a schematic representation of the drug behavior within these polymeric matrices: as explained above, NG-c$^+$ presents high protonation degree (Table 1) and so it is able to retain negatively charged drugs through electrostatic interactions, which do not take place in the case of neutral drugs (Fig. 2A). Otherwise, in the case of NG-u, there are no interactions between the polymeric matrix and drugs loaded within the colloidal dispersion, so they can easily escape driven by diffusion phenomena (Fig. 2B).

The loading percentage of different amounts of drug was checked in order to evaluate the ability of electrostatic interaction between drug and polymers. Table 2 shows the results of drug loading conducted at 37 °C in two different media: aqueous solutions at pH 7.4 and pH 4.5.

While pH 7.4 represents the condition that mimic the classic *in vivo* environment, specific attention is directed toward acidic pH which is typical of some diseases like cancer [42], in order to develop pH-sensitive release systems [43,44]. At pH = 7.4 SF loading is higher for NG-c$^+$ respect to NG-u. This is due to the fact that the loading percentage is influenced by the protonation degree of NGs, induced in their formation: higher protonation allows the retention of a higher amount of negatively charged drug. This assessment is confirmed by the result recorded using the uncharged drug mimetic (RhB): in this case loading percentage is not influenced by protonation degree because no interactions between drug and polymer chains can occur. At pH = 4.5 the protonation of NG-c$^+$ is higher and so the amount of loaded drug is higher than the physiological condition, while NG-u system maintains the same value of entrapped SF. On the contrary, the loading of RhB is extremely low in respect to the case of pH = 7.4: a possible explanation is related to the chemical nature of RhB, which presents a slightly positive charge in acid environment that works as drug-polymer repulsion and therefore the amount of drug that can be loaded decreases.

Once having proved that the NGs systems are able to entrap different types of drugs and evaluated their release profiles, it is necessary to investigate the benefits related to the use of protonated drug delivery systems. SF was chosen for its steric hindrance and its resemblance to many corticosteroids and anti-inflammatory drugs (such as methylprednisolone, ibuprofen, and estradiol) used in pharmacotherapy. Moreover, SF is a sodium salt like several other drugs and in water it is dissociated in fluorescein anion and sodium cation. RhB is another commonly used drug mimetic with the same dimension in order to maintain the same steric hindrance contribution. The latter is a neutral molecule at pH = 7.4 and slightly positive at acid pH: this behavior can be found in several amine-based drugs like lidocaine or trandolapril [30].

The use of these two drug mimetics is also justified by their characteristic functional groups traceable in many drugs containing free carboxylic acid or carbonyl groups, commonly exploited in pharmacotherapy, for example, to hinder SCI secondary effects, CNS damage or cancer side effects [45–48]. SF and RhB, due to the similar steric hindrance, allowed neglecting their dimension effect in order to consider only the role of drug charge contribution.

The percentage of released drug was defined as the ratio between the released amount in the aqueous media and the total amount loaded within the colloidal dispersion.

Table 2
Loading percentages of SF and RhB for NG-c$^+$, NG-u and NG-p$^+$ at different pH.

	pH = 7.4		pH = 4.5	
Nanogel	Loading procedure SF [%]	Loading procedure RhB [%]	Loading procedure SF [%]	Loading procedure RhB [%]
NG-c$^+$	71.8	54.8	78.9	19.7
NG-u	54.3	55.1	55.6	19.9
NG-p$^+$	64.4	54.7	31.8	19.6

In Fig. 3A, SF release profiles from NG-c$^+$ (blue) and NG-u (black) at pH 7.4, are presented. In both cases SF release followed a biphasic pattern characterized by an initial burst release followed by a slower sustained release phase that was observed during 15 days. Referring to NG-c$^+$ nanogels, the electrostatic interactions are able to reduce release rates providing a longer release. Then, to study differences in the diffusion coefficient of SF through NGs we plotted the release against the time to the power of 0.43 ($t^{1/2.3}$, in Fig. 3C), where a linear relationship is indicative of Fickian diffusion. By comparing the slopes in the linear region for NG-c$^+$ and NG-u it is visible that the relative diffusion coefficient is extremely different for the two cases ($p < 0.0001$). For NG-u the data fit linearly for 24 h of release, while for NG-c$^+$, it fit for 5 days. These results confirm that the release from NGs is still mediated by Fickian diffusion and release from NG-c$^+$ is better sustained and controlled than uncharged colloidal dispersion. Moreover, the introduction of high protonation degree allows reducing the burst release from 48% to 28%. The high efficacy of this system is well visible only for charged molecules; indeed, if we consider uncharged drug mimetics (Fig. 3B, D) there are no differences in terms of: drug delivery kinetics, burst release (around 45%) and duration of pure-Fickian diffusion release. These results prove that the higher slowing down of release rates in case of SF is driven by electrostatic interactions between drug molecules and polymeric chains.

Fig. 4A shows the release profiles of SF in NG-c$^+$ (blue) and NG-u (black) at pH 4.5. Also in this case SF release followed a biphasic pattern with an initial burst release and then a slower sustained release phase that was observed during 15 days.

In the case of NG-c$^+$ the electrostatic interactions are able to reduce release rates providing a longer release. In respect to the case plotted in Fig. 3A, at pH = 4.5 SF is characterized by a weaker negative charge than the ionic species presented in the media (H^+ and Cl^-) and it so able to escape very quickly from NGs network. On the contrary, in presence of high protonation the higher charge of the polymeric chains counterbalances the weaker charge of SF and the system is able to reduce the release rate. It is indeed well visible that kinetics obtained with NG-c$^+$ at pH 4.5 is similar to the one measured at pH 7.4. Also burst contribution seems to be independent on the pH of the environment. Then, the differences in the diffusion coefficient of SF through NGs are showed plotting the release against the time to the power of 0.43 ($t^{1/2.3}$, in Fig. 4C). For NG-u the data fit linearly for 4 h of release, while for NG-c$^+$, it fit for all the period investigated. These results confirm that the release from NGs is still mediated by Fickian diffusion and, in particular, the release from NG-c$^+$ is better modulated than the uncharged colloidal dispersion suggesting that this system works very well in acid condition where there is a strong need of selective and controlled drug release [2,43].

As discussed in pH 7.4 environment, also in this condition NG-c$^+$ system presents high efficacy only for charged molecules. Referring to the release of rhodamine, at pH = 4.5 the weak positive charge of RhB works on the opposite way and forces the solute to escape very quickly due to the repulsive forces between loaded drug and polymeric chains. The release of RhB from both NG-u and NG-c$^+$ is almost completed in 4 h with a burst contribution higher than 50%.

3.4. Tuning drug loading and release by tuning counterion

In order to investigate the role of counterion we compared results obtained using hydrochloric acid (NG-c$^+$) presented in Figs. 3 and 4 with the ones obtained with phosphoric acid (NG-p$^+$). H_3PO_4 is a weaker acid and its presence could influence the colloidal dimension, drug loading and drug release rate of charged solutes (such as SF). Nanostructures synthetized using H_3PO_4 were characterized by a diameter of 448 nm and a positive surface density charge, similar to NG-c$^+$ sample as reported in Table 1. These results could be explained considering the strength of the acid: H_3PO_4 is a weak acid and its partial dissociation gave rise to the protonation of PEI in a similar manner to HCl, justifying

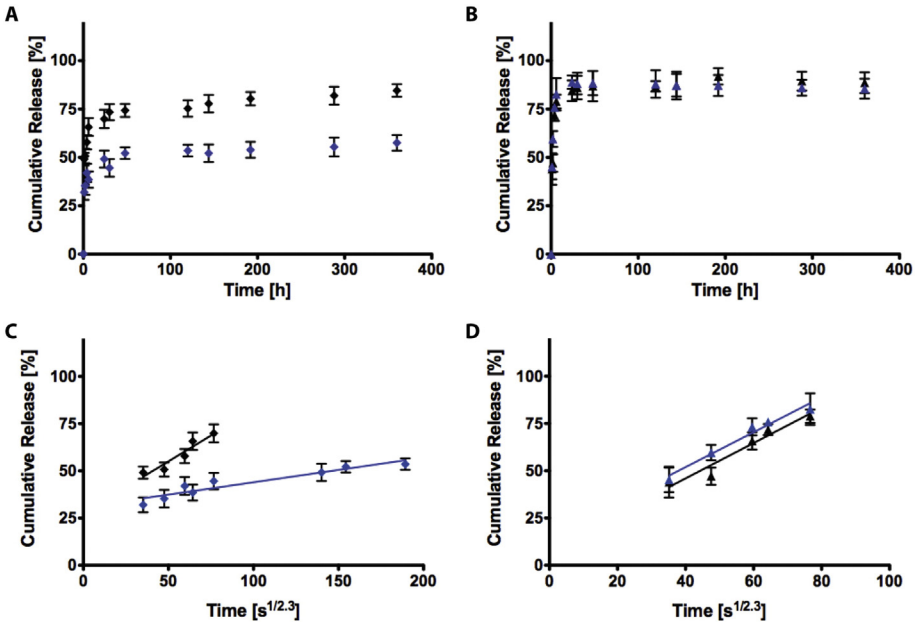

Fig. 3. (A, B) *In vitro* release profile of SF (◆) and RhB (▲) at pH = 7.4 delivered from NG-c$^+$ (blue) and NG-u (black); (C, D) the slope of the SF (◆) and RhB (▲) release at pH = 7.4 from NG-c$^+$ (blue) and NG-u (black) against the variable time expressed as $t^{1/2.3}$ is representative of the Fickian diffusion coefficient of drugs in NGs ($p < 0.0001$ between all of the groups). The diffusion-controlled release is sustained better in NGs loaded with negatively charged drugs. The values are calculated as a percentage with respect to the total mass loaded (mean value ± standard deviation is plotted). (For interpretation of the references to color in this figure legend, the reader is referred to the web version of this article.)

the positive value of ζ-potential. The resulting different intensity of electrostatic interactions, lower than PEI chains in NG-c$^+$ system, enabled the formation of polymeric network with intermediate size between NG-c$^+$ and NG-u.

At pH = 7.4 the loading percentage of SF is 64.4%, lower than value observed for NG-c$^+$ but higher than NG-u (Table 2): this could be explained considering the weaker electrostatic interaction between drug and polymeric chains that occurs in NG-p$^+$. At pH = 4.5 the loading percentage is approximately equal to 31.8%. This value, lower than NG-c$^+$ and NG-u, could be explained considering the weakness of the conjugated base and that, as consequence, SF is more favored to stay outside from the NGs network. In Fig. 5A, SF release profiles at pH 7.4 from NG-c$^+$ (blue) and NG-p$^+$ (red) are presented. In both cases SF release followed a biphasic pattern characterized by an initial burst release and a subsequent slower sustained release phase that was observed during 15 days. Also in the case of NG-p$^+$, electrostatic interactions are able to reduce release rates proving a longer release, comparable with the ones obtained with NG-c$^+$.

The linear relationship (Fig. 5C), typical of Fickian diffusion, is similar between the two case underlining that the counterion does not

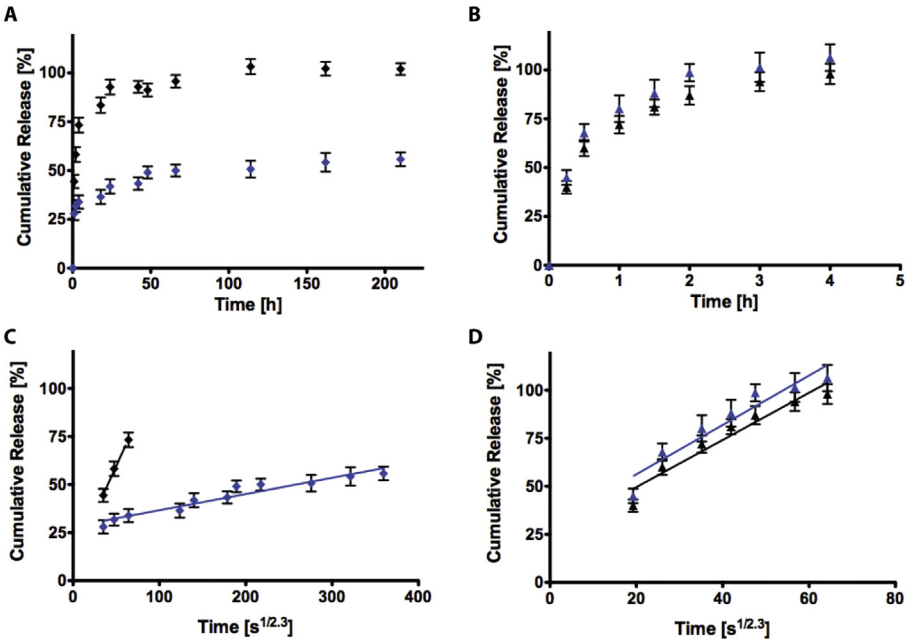

Fig. 4. (A, B) *In vitro* release profile of SF (◆) and RhB (▲) at pH = 4.5 delivered from NG-c$^+$ (blue) and NG-u (black); (C, D) the slope of the SF (◆) and RhB (▲) release at pH = 4.5 from NG-c$^+$ (blue) and NG-u (black) against the variable time expressed as $t^{1/2.3}$ is representative of the Fickian diffusion coefficient of drugs in NGs ($p < 0.0001$ between all of the groups). The values are calculated as a percentage with respect to the total mass loaded (mean value ± standard deviation is plotted). (For interpretation of the references to color in this figure legend, the reader is referred to the web version of this article.)

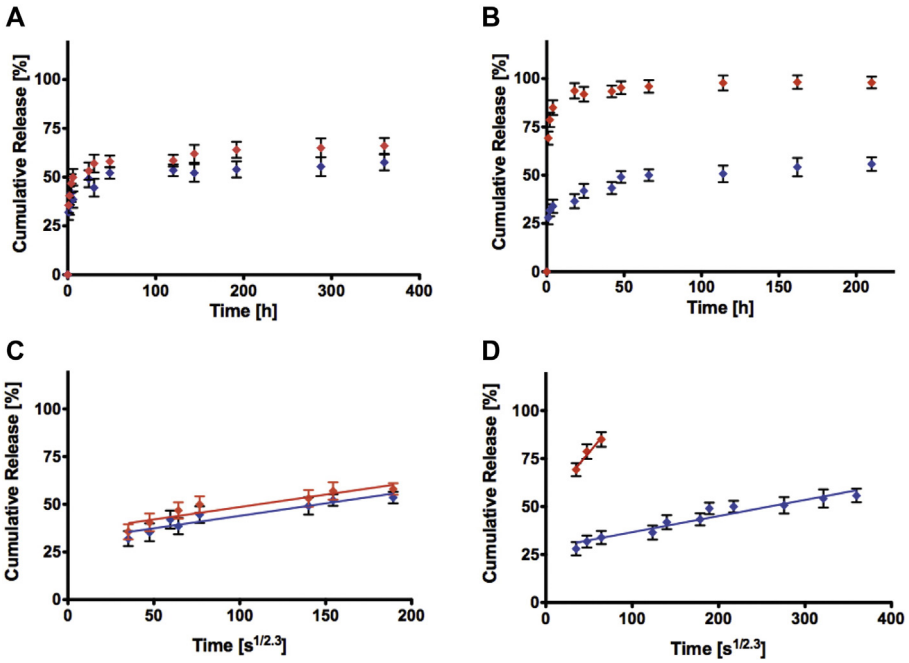

Fig. 5. (A, B) *In vitro* release profile of SF (◆) at pH = 7.4 (A) and pH = 4.5 (B) delivered from NG-c$^+$ (blue) and NG-p$^+$ (red); (C, D) the slope of the SF (◆) release at pH = 7.4 (C) and pH = 4.5 (D) from NG-c$^+$ (blue) and NG-p$^+$ (red) against the square root time is representative of the Fickian diffusion coefficient of drugs in NGs ($p < 0.0001$ between all of the groups). The values are calculated as a percentage with respect to the total mass loaded (mean value ± standard deviation is plotted). (For interpretation of the references to color in this figure legend, the reader is referred to the web version of this article.)

influence very much the release performance of this system. However significant variations appear at pH = 4.5 where a quicker release could be obtained using H_3PO_4 (Fig. 5B, NG-p$^+$) instead of HCl (NG-c$^+$).

A possible explanation lies in the different nature of counterion interacting with the sodium salt form of fluorescein: the interaction among Cl^- and Na^+ is extremely reactive and the anionic form of SF rapidly enters in contact with the protonated component of the nanogel, remaining stably grafted to the polymer network in an electrostatic way, both at pH 7.4 and 4.5, in release media as discussed in Section 3.3. Otherwise, the main form of H_3PO_4 counterion presented at acid pH is H_2PO^{4-} [49,50], which is weaker than Cl^-. The complex between Na^+ cation and H_2PO^{4-} anion is able to form, but it is less stable and requires much more time. The presence in the release acid media of higher amounts of H_2PO^{4-} than within NG-p$^+$ network, probably generates a driving electrostatic interaction force of Na^+ cations outward the nanogel, that maintains their ionic linkage with fluorescein, due to the reduced reactivity with limited amount of counterion H_2PO^{4-} available within the nanogel, and this results as quicker diffusion of SF and its fast release in an acid environment. Indeed, SF release seems to be completed within 24 h in case of NG-p$^+$, whereas NG-c$^+$ sample shows that only 35% of drug mimetic escaped from the polymeric network in the same period of time (Fig. 5B).

4. Conclusions

Control over the release rate is essential for the success of sustained drug delivery devices. Moreover, the possibility to provide systems with the same composition but able to increase or reduce release rates, is a pivotal point in biomedical field. We hypothesized that the tuning of electrostatic interactions between drugs and polymer chains could be very efficient for this purpose. In this direction we synthesized NGs based on PEG-PEI, suitable for biomedical applications, with different protonation degrees and we studied release performances with charged (SF) and uncharged (RhB) drug mimetics. Electrostatic interactions are able to limit drug diffusion during time both at pH = 7.4 and in acid condition (pH = 4.5) typical of cancer environment. In addition, also the role of counter ion was investigated and taken into account in order to have a finer tunability of our formulation. The absence of covalent bonds between loaded drugs and polymers is the key point of this approach that can reduce or increase Fickian flow without any conformational modification of the loaded solute (drug). Thus, such formulated colloids can be profitably adopted when active agents should be released with independent kinetics.

Acknowledgments

Authors would like to thank Dr. Chiara Allegretti for fruitful discussion.

References

[1] S. Papa, F. Rossi, R. Ferrari, A. Mariani, M. De Paola, I. Caron, F. Fiordaliso, C. Bisighini, E. Sammali, C. Colombo, M. Gobbi, M. Canovi, J. Lucchetti, M. Peviani, M. Morbidelli, G. Forloni, G. Perale, D. Moscatelli, P. Veglianese, Selective nanovector mediated treatment of activated proinflammatory microglia/macrophages in spinal cord injury, ACS Nano 7 (2013) 9881–9895.
[2] K. Ulbrich, K. Hola, V. Subr, A. Bakandritsos, J. Tucek, R. Zboril, Targeted drug delivery with polymers and magnetic nanoparticles: covalent and noncovalent approaches, release control, and clinical studies, Chem. Rev. 116 (2016) 5338–5431.
[3] H. Zhang, Y. Zhai, J. Wang, G. Zhai, New progress and prospects: the application of nanogel in drug delivery, Mater. Sci. Eng. C 60 (2015).
[4] D. Depan, R.D.K. Misra, Hybrid nanostructured drug carrier with tunable and controlled drug release, Mater. Sci. Eng. C 32 (2012) 1704–1709.
[5] K. Park, Controlled drug delivery systems: past forward and future back, J. Control. Release 190 (2014) 3–8.
[6] M.W. Tibbitt, J.E. Dahlman, R. Langer, Emerging frontiers in drug delivery, J. Am. Chem. Soc. 138 (2016) 704–717.
[7] F. Rossi, G. Perale, S. Papa, G. Forloni, P. Veglianese, Current options for drug delivery to the spinal cord, Expert Opin. Drug Deliv. 10 (2013) 385–396.
[8] N.A. Peppas, Historical perspective on advanced drug delivery: how engineering design and mathematical modeling helped the field mature, Adv. Drug Deliv. Rev. 65 (2013) 5–9.
[9] M.W. Tibbitt, C.B. Rodell, J.A. Burdick, K.S. Anseth, Progress in material design for biomedical applications, Proc. Natl. Acad. Sci. U. S. A. 112 (2015) 14444–14451.
[10] M. Zafar, T. Shah, A. Rawal, E. Siores, Preparation and characterisation of thermoresponsive nanogels for smart antibacterial fabrics, Mater. Sci. Eng. C 40 (2014) 135–141.
[11] P. Kaur, T. Garg, G. Rath, R.S.R. Murthy, A.K. Goyal, Surfactant-based drug delivery systems for treating drug-resistant lung cancer, Drug Deliv. 23 (2016) 727–738.
[12] L. Yang, P. Alexandridis, Physicochemical aspects of drug delivery and release from polymer-based colloids, Curr. Opin. Colloid Interface Sci. 5 (2000) 132–143.

[13] J. Nicolas, S. Mura, D. Brambilla, N. Mackiewicz, P. Couvreur, Design, functionalization strategies and biomedical applications of targeted biodegradable/biocompatible polymer-based nanocarriers for drug delivery, Chem. Soc. Rev. 42 (2013) 1147–1235.
[14] I. Posadas, S. Monteagudo, V. Cena, Nanoparticles for brain-specific drug and genetic material delivery, imaging and diagnosis, Nanomedicine 11 (2016) 833–849.
[15] F. Rossi, F. Castiglione, M. Ferro, M. Moioli, A. Mele, M. Masi, The role of drug–drug interactions in hydrogel delivery systems: experimental and model study, ChemPhysChem 17 (2016) 1615–1622.
[16] E. Mauri, F. Rossi, A. Sacchetti, Tunable drug delivery using chemoselective functionalization of hydrogels, Mater. Sci. Eng. C 61 (2016) 851–857.
[17] M.M. Pakulska, I.E. Donaghue, J.M. Obermeyer, A. Tuladhar, C.K. McLaughlin, T.N. Shendruk, M.S. Shoichet, Encapsulation-free controlled release: electrostatic adsorption eliminates the need for protein encapsulation in PLGA nanoparticles, Sci. Adv. 2 (2016), e1600519.
[18] M.L. Chang, F. Zhang, T. Wei, T.T. Zuo, Y.Y. Guan, G.M. Lin, W. Shao, Smart linkers in polymer-drug conjugates for tumor-targeted delivery, J. Drug Target. 24 (2016) 475–491.
[19] K. Vulic, M.S. Shoichet, Tunable growth factor delivery from injectable hydrogels for tissue engineering, J. Am. Chem. Soc. 134 (2012) 882–885.
[20] D. Ossipov, S. Kootala, Z. Yi, X. Yang, J. Hilborn, Orthogonal chemoselective assembly of hyaluronic acid networks and nanogels for drug delivery, Macromolecules 46 (2013) 4105–4113.
[21] F. Rossi, M. van Griensven, Tissue Eng. Part A 20 (2014) 2043–2051.
[22] S. Beke, R. Barenghi, B. Farkas, I. Romano, L. Korösi, S. Scaglione, F. Brandi, Improved cell activity on biodegradable photopolymer scaffolds using titanate nanotube coatings, Mater. Sci. Eng. C 44 (2014) 38–43.
[23] N. Yoneki, T. Takami, T. Ito, R. Anzai, K. Fukuda, K. Kinoshita, S. Sonotaki, Y. Murakami, One-pot facile preparation of PEG-modified PLGA nanoparticles: effects of PEG and PLGA on release properties of the particles, Colloids Surf. A Physicochem. Eng. Asp. 469 (2015) 66–72.
[24] E. Mauri, I. Moroni, L. Magagnin, M. Masi, A. Sacchetti, F. Rossi, Comparison between two different click strategies to synthesize fluorescent nanogels for therapeutic applications, React. Funct. Polym. 105 (2016) 35–44.
[25] M. Santoro, P. Marchetti, F. Rossi, G. Perale, F. Castiglione, A. Mele, M. Masi, Smart approach to evaluate drug diffusivity in injectable agar-carbomer hydrogels for drug delivery, J. Phys. Chem. B 115 (2011) 2503–2510.
[26] T. Casalini, M. Salvalaglio, G. Perale, M. Masi, C. Cavallotti, Diffusion and aggregation of sodium fluorescein in aqueous solutions, J. Phys. Chem. B 115 (2011) 12896–12904.
[27] G. Perale, P. Arosio, D. Moscatelli, V. Barri, M. Muller, S. Maccagnan, M. Masi, A new model of resorbable device degradation and drug release: transient 1-dimension diffusional model, J. Control. Release 136 (2009) 196–205.
[28] Y.Z. Wang, B.C. Wang, W.L. Qiao, T.Y. Yin, A novel controlled release drug delivery system for multiple drugs based on electrospun nanofibers containing nanoparticles, J. Pharm. Sci. 99 (2010) 4805–4811.
[29] Z. Yu, M. Yu, Z.B. Zhang, G. Hong, Q.Q. Xiong, Bovine serum albumin nanoparticles as controlled release carrier for local drug delivery to the inner ear, Nanoscale Res. Lett. 9 (2014).
[30] R.Y. Zhang, M. Hummelgard, G. Lv, H. Olin, Real time monitoring of the drug release of rhodamine B on graphene oxide, Carbon 49 (2011) 1126–1132.
[31] S. Vinogradov, E. Batrakova, A. Kabanov, Poly(ethylene glycol)-polyethyleneimine nanogel (TM) particles: novel drug delivery systems for antisense oligonucleotides, Colloids Surf. B 16 (1999) 291–304.
[32] P.C. Griffiths, A. Paul, P. Stilbs, E. Petterson, Charge on poly(ethylene imine): comparing electrophoretic NMR measurements and pH titrations, Macromolecules 38 (2005) 3539–3542.
[33] M. Neu, D. Fischer, T. Kissel, Recent advances in rational gene transfer vector design based on poly(ethylene imine) and its derivatives, J. Gene Med. 7 (2005) 992–1009.
[34] R. Meszaros, L. Thompson, M. Bos, P. de Groot, Adsorption and electrokinetic properties of polyethylenimine on silica surfaces, Langmuir 18 (2002) 6164–6169.
[35] Y. Fukumoto, Y. Obata, K. Ishibashi, N. Tamura, I. Kikuchi, K. Aoyama, Y. Hattori, K. Tsuda, Y. Nakayama, N. Yamaguchi, Cost-effective gene transfection by DNA compaction at pH 4.0 using acidified, long shelf-life polyethylenimine, Cytotechnology 62 (2010) 73–82.
[36] S.V. Vinogradov, T.K. Bronich, A.V. Kabanov, Nanosized cationic hydrogels for drug delivery: preparation, properties and interactions with cells, Adv. Drug Deliv. Rev. 54 (2002) 135–147.
[37] S.V. Vinogradov, E.V. Batrakova, A.V. Kabanov, Nanogels for oligonucleotide delivery to the brain, Bioconjug. Chem. 15 (2004) 50–60.
[38] L. Shang, K. Nienhaus, G.U. Nienhaus, Engineered nanoparticles interacting with cells: size matters, J. Nanobiotechnol. 12 (2014).
[39] L. Shang, L.X. Yang, J. Seiter, M. Heinle, G. Brenner-Weiss, D. Gerthsen, G.U. Nienhaus, Nanoparticles interacting with proteins and cells: a systematic study of protein surface charge effects, Adv. Mater. Interfaces 1 (2014).
[40] N. Sahiner, W.T. Godbey, G.L. McPherson, V.T. John, Microgel, nanogel and hydrogel-hydrogel semi-IPN composites for biomedical applications: synthesis and characterization, Colloid Polym. Sci. 284 (2006) 1121–1129.
[41] C. Colombo, L. Galletti, M. Lepri, I. Caron, L. Magagnin, P. Veglianese, F. Rossi, D. Moscatelli, Multidrug encapsulation within self-assembled 3D structures formed by biodegradable nanoparticles, Eur. Polym. J. 68 (2015) 216–225.
[42] X.L. Wei, Q. Luo, L. Sun, X. Li, H.Y. Zhu, P.J. Guan, M. Wu, K. Luo, Q.Y. Gong, Enzyme- and pH-sensitive branched polymer-doxorubicin conjugate-based nanoscale drug delivery system for cancer therapy, ACS Appl. Mater. Interfaces 8 (2016) 11765–11778.
[43] D.S. Spencer, A.S. Puranik, N.A. Peppas, Intelligent nanoparticles for advanced drug delivery in cancer treatment, Curr. Opin. Chem. Eng. 7 (2015) 84–92.
[44] S. Dutta, S. Parida, C. Maiti, R. Banerjee, M. Mandal, D. Dhara, Polymer grafted magnetic nanoparticles for delivery of anticancer drug at lower pH and elevated temperature, J. Colloid Interface Sci. 467 (2016) 70–80.
[45] Y.T. Kim, J.M. Caldwell, R.V. Bellamkonda, Nanoparticle-mediated local delivery of methylprednisolone after spinal cord injury, Biomaterials 30 (2009) 2582–2590.
[46] D.W. Brann, K. Dhandapani, C. Wakade, V.B. Mahesh, M.M. Khan, Neurotrophic and neuroprotective actions of estrogen: basic mechanisms and clinical implications, Steroids 72 (2007) 381–405.
[47] C. Rodriguez-Tenreiro, C. Alvarez-Lorenzo, A. Rodriguez-Perez, A. Concheiro, J.J. Torres-Labandeira, Estradiol sustained release from high affinity cyclodextrin hydrogels, Eur. J. Pharm. Biopharm. 66 (2007) 55–62.
[48] J.L. Arias, F. Linares-Molinero, V. Gallardo, A.V. Delgado, Study of carbonyl iron/poly(butylcyanoacrylate) (core/shell) particles as anticancer drug delivery systems — loading and release properties, Eur. J. Pharm. Sci. 33 (2008) 252–261.
[49] E.B.R. Prideaux, A.T. Ward, L.—The dissociation constants of phosphoric acid, J. Chem. Soc. Trans. 125 (1924) 423–426.
[50] D.R. Migneault, R.K. Forcé, Dissociation constants of phosphoric acid at 25 °C and the ion pairing of sodium with orthophosphate ligands at 25 °C, J. Solut. Chem. 17 (1988) 987–997.